Spectroscopic Analysis of a Biomimetic Model of TyrZ Function in PSII

ARTICLE *in* THE JOURNAL OF PHYSICAL CHEMISTRY B · SEPTEMBER 2015

Impact Factor: 3.3 · DOI: 10.1021/acs.jpcb.5b05298 · Source: PubMed

THE JOURNAL OF PHYSICAL CHEMISTRY B

Article

pubs.acs.org/JPCB

Spectroscopic Analysis of a Biomimetic Model of Tyr_Z Function in PSII

Janneke Ravensbergen,[†] Antaeres Antoniuk-Pablant,[‡] Benjamin D. Sherman,[‡] Gerdenis Kodis,[‡] Jackson D. Megiatto, Jr.,[‡] Dalvin D. Méndez-Hernández,[‡] Raoul N. Frese,[†] Rienk van Grondelle,[†] Thomas A. Moore,[‡] Ana L. Moore,[‡] Devens Gust,[‡] and John T. M. Kennis*[,†]

[†]Department of Physics and Astronomy, Faculty of Sciences, VU University, De Boelelaan 1081, 1081 HV Amsterdam, The Netherlands

[‡]Department of Chemistry & Biochemistry and Center for Bioenergy and Photosynthesis, Arizona State University, Tempe, Arizona 85287-1605, United States

Supporting Information

ABSTRACT: Using natural photosynthesis as a model, bio-inspired constructs for fuel generation from sunlight are being developed. Here we report the synthesis and time-resolved spectroscopic analysis of a molecular triad in which a porphyrin electron donor is covalently linked to both a cyanoporphyrin electron acceptor and a benzimidazole−phenol model for the Tyr_Z-D_1His190 pair of PSII. A dual-laser setup enabled us to record the ultrafast kinetics and long-living species in a single experiment. From this data, the photophysical relaxation pathways were elucidated for the triad and reference compounds. For the triad, quenching of the cyanoporphyrin singlet excited state lifetime was interpreted as photoinduced electron transfer from the porphyrin to the excited cyanoporphyrin. In contrast to a previous study of a related molecule, we were unable to observe subsequent formation of a long-lived charge separated state involving the benzimidazole−phenol moiety. The lack of detection of a long-lived charge separated state is attributed to a change in energetic landscape for charge separation/recombination due to small differences in structure and solvation of the new triad.

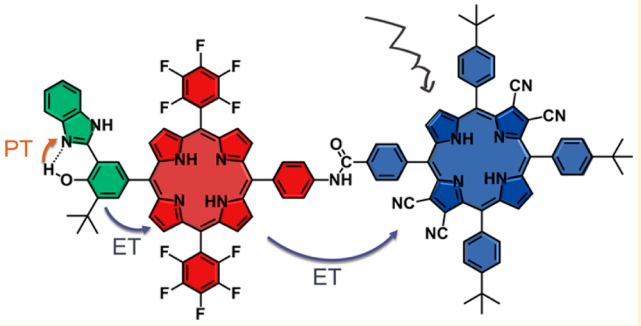

INTRODUCTION

Photosynthesis uses molecular chromophores to capture sunlight and drive chemical reactions. In order to prevent rapid recombination of the charge separated state formed after excitation, the radical anion and radical cation are spatially separated over several nanometers by sequential electron transfer steps. In oxygenic photosynthesis, electron transfer from the oxygen evolving complex (OEC)—a manganese and calcium cluster—to the primary donor is mediated by a proton coupled electron transfer (PCET) step.[1] This PCET mechanism in natural photosynthesis is believed to be key for bridging the time scales of the initial electron transfer dynamics and multielectron catalysis.[2]

In photosystem II (PSII) of plants, excitation energy is transferred to the reaction center that contains four chlorophyll and two pheophytin molecules ($Pheo_{D1}$, Chl_{D1}, P_{D1}, P_{D2}, Chl_{D2}, and $Pheo_{D2}$). Excitation of the PSII reaction center leads to collective excited states followed by multiple charge separation pathways either driven by exciton states largely localized on Chl_{D1} or on P_{D1}−P_{D2} chromophores, which ultimately lead to $P_{D1}^{\bullet+}Pheo_{D1}^{\bullet-}$. The $P_{D1}^{\bullet+}$ cation, also referred to as $P680^{\bullet+}$, is reduced by the tyrosine Z residue (Tyr_Z-OH) via a PCET mechanism that involves an electron transfer reaction to $P_{D1}^{\bullet+}$ and a proton transfer to a hydrogen-bonded histidine residue (D_1His190). The oxidized and deprotonated Tyr_Z-$O^{\bullet}$ species is reduced by the OEC, a process that is coupled to reprotonation of the tyrosine residue to regenerate Tyr_Z-OH. After four oxidation steps, two water molecules are oxidized by the OEC and O_2 is formed.[3−5]

Using natural photosynthesis as inspiration, constructs for fuel generation from sunlight are being developed. These approaches have also increased our understanding of natural photosynthesis. Various donor−acceptor dyads have been shown to undergo photoinduced electron transfer processes. However, they typically recombine on the picosecond to nanosecond time scale, and most are thermodynamically not capable of water oxidation.[6−11] In other, more complex constructs longer recombination lifetimes have been demonstrated, including some in which PCET is involved.[2,12−22]

Here we report a spectroscopic study of a triad that consists of two porphyrins and a benzimidazole−phenol moiety (BiPhOH) (Figure 1). One of the porphyrins (PF_{10}) has two

Received: June 3, 2015
Revised: August 28, 2015
Published: September 1, 2015

DOI: 10.1021/acs.jpcb.5b05298
J. Phys. Chem. B 2015, 119, 12156−12163

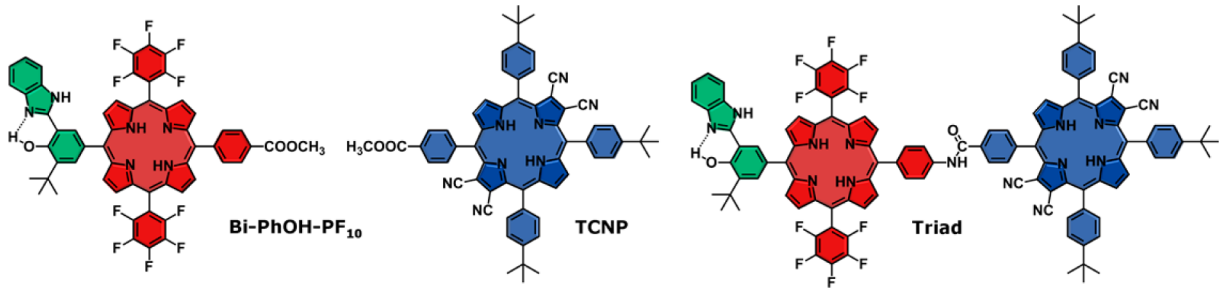

Figure 1. Structures of investigated compounds.

pentafluorophenyl groups at *meso*-positions, and the other porphyrin (TCNP) has four cyano groups at the *beta*-positions of the macrocycle. The substituents on the porphyrins are designed to favor electron transfer from PF_{10} to TCNP to form Bi-PhOH-$PF_{10}^{\bullet+}$-$TCNP^{\bullet-}$, followed by electron transfer from Bi-PhOH to $PF_{10}^{\bullet+}$. The Bi-PhOH moiety is designed to mimic the PCET performed by the tyrosine−histidine pair of PSII. The phenol group of Bi-PhOH forms a strong hydrogen bond to one of the nitrogen atoms of the benzimidazole moiety. Upon oxidation, the electron transfer is accompanied by proton transfer to form the BiH^{+}-$PhO^{\bullet}$ species.[20−22] This PCET mechanism is expected to stabilize the targeted final charge separated state: BiH^{+}-$PhO^{\bullet}$-PF_{10}-$TCNP^{\bullet-}$.

We provide a detailed time-resolved spectroscopic analysis on the triad and two reference compounds in benzonitrile and acetonitrile with a broadband probe in the visible and near-IR. The reference compounds studied in parallel with the triad are TCNP and Bi-PhOH-PF_{10} (Figure 1). A dual-laser setup enabled us to record the ultrafast kinetics and long-living species in a single experiment. From this data the photophysical pathways were elucidated for the triad and reference compounds.

The triad investigated here is similar, but not identical, to the one reported previously by Megiatto et al.,[18] which has two *tert*-butyl groups in the 3,5-positions of each of the three of the *meso*-phenyl groups on the TCNP moiety, instead of a single *tert*-butyl group in the 4-position of each of three *meso*-phenyl groups. For the previously studied triad, a charge separated state with lifetime of 3.8 μs and approximately 50% yield was reported. We compare our findings with the results reported in that study.

MATERIALS AND METHODS

Synthesis. All chemicals were purchased from Aldrich, Alfa Aesar or Acros and were used without further purification. Solvents were obtained from EM Science and were used as received unless otherwise noted. Dimethylacetamide was stirred with BaO for 24 h, refluxed over BaO for 1 h, and distilled under reduced pressure before use. $Zn(OAc)_2$, 1,1′-bis-(diphenylphosphino)ferrocene, and Zn dust were dried under vacuum overnight. All glassware was oven-dried overnight before use. Thin layer chromatography (TLC) was performed with silica gel coated glass plates from Analtech. Column chromatography was carried out using Silicycle silica gel 60 with 230−400 mesh. The ^{1}H NMR spectra were recorded on a Varian spectrometer at 400 or 500 MHz. NMR samples were prepared in deuteriosolvents with tetramethylsilane as an internal reference using a Wilmad 528-PP 5 mm NMR tube. Deuterated chloroform was distilled from CaH. Mass spectra were obtained with a matrix-assisted laser desorption/ionization time-of-flight spectrometer (MALDI-TOF), using (1*E*,3*E*)-1,4-diphenylbuta-1,3-diene (DPB), cyano-4-hydroxycinnamic acid (CCA), or terthiophene as a matrix. The reported mass is of the most abundant isotopic ratio observed. To facilitate comparison, calculated values of the expected most abundant isotopic ratio are listed after the experimental result. The Bi-PhOH-PF_{10} dyad was synthesized following the procedures reported in previous works.[18−20]

Synthesis of 2,3,12,13-Tetracyano-5-(4-methoxycarbonyl)-10,15,20-tris(4-tert-butylphenyl)porphyrin (TCNP). This compound was synthesized from Zn(II) 2,3,12,13-tetrabromo-5-(4-methoxycarabonyl)-10,15,20-tris(4-*tert*-butylphenyl)porphyrin derivative[20,23] and $Zn(CN)_2$ following the palladium-mediated cyanation procedure recently developed at Arizona State University. In a Schlenk flask equipped with a magnetic stir bar, the Zn(II) tetrabromoporphyrin derivative (350 mg, 0.287 mmol), tris(dibenzylideneacetone)-dipalladium(0) (210 mg, 0.229 mmol), 1,1′-bis(diphenylphosphino)ferrocene (255 mg, 0.460 mmol), zinc acetate (16 mg, 0.09 mmol), Zn dust (9 mg, 0.1 mmol), and zinc cyanide (81 mg, 0.69 mmol) were dissolved in 40 mL of oxygen-free dimethylacetamide. The Schlenk flask was placed in an oil bath which was brought to a temperature of 115 °C, and the reaction mixture was stirred under argon for 20 h. The reaction mixture was cooled to room temperature, and dichloromethane (60 mL) was added. The resulting solution was washed five times with water (100 mL), the organic layer was collected, and the solvent was removed by distillation under reduced pressure. The product was purified by column chromatography on silica gel, using 20% ethyl acetate in toluene as the eluent. A final purification was done by recrystallization from dichloromethane and hexane to afford the target porphyrin as purple crystals (115 mg, ∼40% yield). ^{1}H NMR (400 MHz, $CDCl_3$, δ ppm): 8.73−8.86 (m, 3 H, pyrrolic H), 8.60 (d, J = 4.8 Hz, 1 H, pyrrolic H), 8.43 (d, J = 8.3 Hz, 2 H, Ar), 8.17 (d, J = 8.3 Hz, 2 H, Ar), 7.89−8.02 (m, 6 H, Ar), 7.67−7.83 (m, 6 H, Ar), 4.09 (s, 3 H, methoxy H), 1.60 (s, 27 H, *tert*-butyl H). UV−vis, λ_{max} (nm, 2% MeOH in CH_2Cl_2): 443, 458, 657, 677. MALDI-TOF-MS m/z: calcd for $C_{62}H_{50}N_8O_2Zn$ 1002.34; obsd 1002.67 $[M]^+$.

This isolated porphyrin (0.012 g, 0.012 mmol) was dissolved in 10 mL of dry dichloromethane, and 10 mL of trifluoroacetic acid was added under an inert atmosphere. The brown reaction mixture was stirred for 30 min at room temperature. The crude product was neutralized with triethylamine, washed with water (2 × 10 mL), dried over sodium sulfate, filtered through paper, and concentrated under reduced pressure. Final purification was achieved by flash chromatography (SiO_2) using dichloromethane as eluent to afford the TCNP derivative as a bluish-green solid in quantitative yield (0.012 g). ^{1}H NMR (400 MHz,

DOI: 10.1021/acs.jpcb.5b05298
J. Phys. Chem. B 2015, 119, 12156−12163

$CDCl_3$, δ ppm): 9.01 (m, 3H, pyrrolic protons); 8.86 (dd, 1H, pyrrolic proton); 8.49 (d, J = 8.3 Hz, 2 H, Ar), 8.26 (d, J = 8.3 Hz, 2 H, Ar), 7.89−8.02 (m, 6 H, Ar), 7.67−7.83 (m, 6 H, Ar), 4.10 (s, 3 H, methoxy H), 1.53 (s, 27 H, *tert*-butyl H); −2.43 (s, 1H, NH); −2.45 (s, 1H, NH). MALDI-TOF-MS (positive mode, m/z): calcd for $C_{62}H_{52}N_8O_2$ 940.42; obsd 940.78 $[M]^+$.

Synthesis of the Triad.[20] Compounds 5,15-bis(2,3,4,5,6-pentafluorophenyl)-10-(4-aminophenyl)-20-[2′-(3-*tert*-butyl-2″-hydroxyphenyl)benzimidazole]porphyrin (0.006 g, 6.00 μmol) and 2,3,12,13-tetracyano-5-(4-carboxyphenyl)-10,15,20-tris(4-*tert*-butylphenyl)porphyrin (0.006 g, 6.6 μmol) were dissolved in 3 mL of dichloromethane under an inert atmosphere. Dimethylaminopyridine (DMAP) (0.002 g, 0.01 mmol) and 1-ethyl-3-(3-(dimethylamino)propyl)carbodiimide (0.002 g, 8.22 μmol) were added, and the reaction mixture was stirred at room temperature for 12 h. The crude mixture was diluted with 20 mL of dichloromethane, washed with water (3 × 20 mL), dried over $MgSO_4$, filtered through paper, and concentrated. Final purification was achieved by column chromatography (SiO_2) using a gradient of hexanes/dichloromethane as eluent to afford the target triad as a greenish-purple solid (0.007 g, ∼60% yield). The ^{1}H NMR assignment is shown in Figure SI 1. MALDI-TOF-MS (positive mode, m/z): calcd for $C_{116}H_{81}F_{10}N_{15}O_2$ 1906.97; obsd 1907.15 $[M]^+$.

Spectroscopy. Room-temperature steady state absorption spectra were recorded on a PerkinElmer Lambda 40 UV/vis spectrometer. Both steady state and transient absorption spectra were recorded using a 1 mm quartz cuvette. The solvents were not deoxygenated.

Transient absorption spectroscopy was performed on a setup using two electronically synchronized amplified Ti:sapphire laser systems (Legend and Libra, Coherent, Santa Clara, CA) as described previously.[24] The amplifiers were seeded by a single 80 MHz oscillator (Vitesse, Coherent) and pumped with separate pump lasers (Evolution, Coherent). Both lasers have an 800 nm output at a repetition rate of 1 kHz. The output power is 3.0 W for the Legend and 4.5 W for the Libra. The output of the Legend was used to drive an optical parametric amplifier (OperA SOLO, TOPAS, Coherent) with which the excitation wavelength was set. TCNP and triad were excited at 730 nm, and the Bi-PhOH-PF_{10} compound was excited at 511 nm. Excitation energies of 100−200 nJ were used at a spot size of ∼300 μm.

A broadband probe beam was generated by focusing part of the output of the Libra on a CaF_2 or sapphire plate. In acetonitrile (ACN) the visible part of the spectrum was recorded in two measurements with partly overlapping probe windows, and the data were analyzed simultaneously. In benzonitrile the visible part data were recorded in one measurement and the near-IR in another; these probe windows were not overlapping. As a result, variation in pump power intensity might lead to differences in spectral amplitude between the VIS and near-IR. The transient absorption signal was acquired in a multichannel fashion by spectrally dispersing the probe through a spectrograph projecting it on a 256-element diode array detector.[25] The instrument response function had a width of 100 fs (full width at half-maximum).

The time difference between pump and probe was controlled in two ways. An optical delay line was used for delays of the pump beam in the fs to 3.5 ns regime. Delay steps of 12.5 ns were generated by selection and amplification of consecutive seed pulses of the oscillator. The timing of the amplification process of the Libra was controlled by a signal delay generator (SDG Elite, Coherent). A second signal delay generator—one that synchronizes with the first—governed the timing of the Legend (SDG, Coherent). By varying the triggering of the second SDG with respect to the first, delays of the probe up to 0.8 ms were achieved. Both delay methods were applied simultaneously, addressing the fs to ms range in a single experiment.

Global analysis of the transient absorption data was performed using the Glotaran program.[26] In global analysis all wavelengths are analyzed simultaneously, and a set of common time constants and spectra is produced.[27,28] Here, we present both sequentially interconverting and parallel decaying (sum-of-exponentials) models. In a sequential analysis (1 → 2 → 3 → ...) the numbers indicate evolution-associated difference spectra (EADS) that interconvert with successive monoexponential decay times, each of which can be regarded as the lifetime of each EADS. The first EADS corresponds to the time-zero difference spectrum. The first EADS evolves into the second EADS with time constant τ_1, which in turn evolves in the third EADS with time constant τ_2, etc. This procedure clearly visualizes the evolution of the excited and intermediate states of the system. In general, the EADS may well reflect mixtures of difference spectra of pure electronic states, which may arise from heterogeneous ground states or branching at any point in the photoinduced evolution.[29−31] The parallel sum-of-exponentials decay scheme produces decay-associated difference spectra (DADS). DADS indicate the spectral changes that occur with their associated time constants. In essence, DADS denote the spectral differences that occur on going from one EADS to another. It is important to note that sequential analysis is mathematically equivalent to a parallel analysis. The analysis program calculates both EADS and DADS and the time constants that follow from the analysis apply to both.[32] For a more detailed description of global analysis we refer to Van Stokkum et al.[27,28]

RESULTS AND DISCUSSION

Steady State Absorption Spectroscopy. Figure 2 shows the steady state absorption spectra of the compounds in benzonitrile. TCNP shows a split Soret band with maxima at 444 and 458 nm. The Q-bands are found at 520, 556, 601, 674, and 738 nm. Bi-PhOH-PF_{10} displays a single Soret band at 424 nm and Q-bands at 514, 549, 589, and 644 nm that originate from the PF_{10} part of the compound. The triad contains Soret and Q-bands from both porphyrin derivatives. In acetonitrile

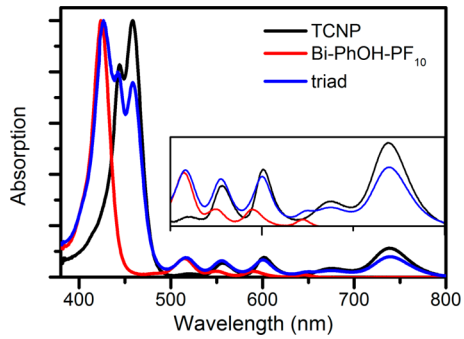

Figure 2. Absorption spectra of TCNP, Bi-PhOH-PF_{10}, and the triad in benzonitrile, scaled to the maximum value. The inset shows a magnification of the absorption in the 500−800 nm region.

DOI: 10.1021/acs.jpcb.5b05298
J. Phys. Chem. B 2015, 119, 12156−12163

the absorption spectra of the three compounds are similar but slightly blue-shifted (Figure SI 2).

Transient Absorption Spectroscopy. The photophysical processes of the compounds were studied by transient absorption spectroscopy in benzonitrile and acetonitrile. The transient absorption data were analyzed globally and presented in the form of EADS here and in the form of DADS and additional EADS in the Supporting Information. A description of global analysis method is given in the Materials and Methods section. Raw transient absorption data are presented in Figures SI 10−15.

TCNP. The TCNP compound was excited at the lowest-energy absorption band with a 730 nm pump pulse. Figure 3 shows the EADS of TCNP in benzonitrile; the DADS are given in Figure SI 3. The initial EADS (black) rises with the instrument response of 100 fs. The positive contribution to the spectrum originates from excited state absorption (ESA). The initial spectrum shows ESA in both the VIS and near-IR. Negative contributions originate from ground state bleach (GSB) at the absorption bands discussed in the previous section and stimulated emission (SE) at the low energy side of the Q-band. Four components with time constants of 2.1 ps, 73 ps, 1.7 ns, and 698 ns are needed for a sufficient fit of the data.

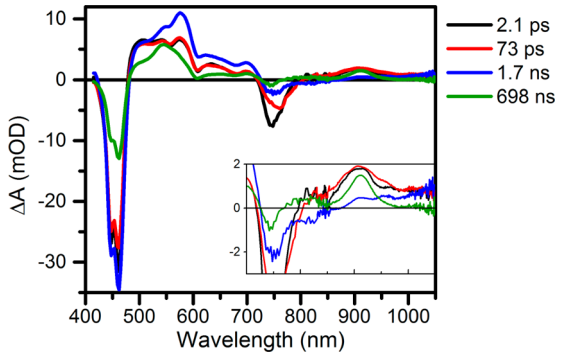

Figure 3. EADS of TCNP in benzonitrile upon 730 nm excitation. The inset shows a magnification of the Δ*A* axis in the 700−1050 nm region.

The first relaxation process occurs with a time constant of 2.1 ps and is shown by the evolution of the first EADS (black) into the second EADS (red). We observe a band-shift of the Q-band and an increase of ESA around 940 nm. In the second process (red to blue, 73 ps) the amplitude of the SE band decreases, while the amplitude of ESA increases in the VIS and decreases in the near-IR. Note that the apparent decrease of stimulated emission might by caused by a red-shift of this band or an increase of the overlapping positive ESA. The resulting blue EADS has a maximum at 580 nm; the band at 910 nm has almost disappeared. The spectral changes observed for the 2.1 and 73 ps evolutions are typical for solvation and relaxation processes. Because of the change in energetic landscape upon solvation and relaxation, transitions to higher lying states can gain (in the visible in this case) or lose (in the 910 nm band) strength. Typically, these processes occur on the subpicosecond to early picosecond time scale. The 73 ps time scale found here and similar time scale for the tetracyanoporphyrin reported by Megiatto et al. are much longer.[18] Such slow relaxation processes have been reported previously by Sazanovich et al. for porphyrins with substituents on the *beta*-positions of the macrocycle and were explained as relaxation in a complex excited state manifold due to nonplanar conformations.[33] The quality of the fit is not very sensitive to the values of the first two processes; presumably the solvation and relaxation occur on a range of time scales that are not all separated in the analysis.

The third EADS (blue) is assigned to the relaxed singlet excited state and evolves with a time constant of 1.7 ns to the final EADS (green), reflecting the triplet state. The triplet spectrum has maxima at 545 and 910 nm and a lifetime of 698 ns in air-saturated solution. The triplet yield is roughly estimated to be 37%, based on the amplitude of the Soret band GSB.

For TCNP in acetonitrile (probed in VIS) similar kinetics are obtained (Figure SI 4), with time constants of 710 fs, 11 ps, 1.2 ns, and 524 ns. The triplet yield in acetonitrile is estimated to be 39%.

Bi-PhOH-PF10. The Bi-PhOH-PF_{10} compound was excited in the highest energy Q-band at 511 nm. The results of global analysis of Bi-PhOH-PF_{10} in benzonitrile are shown in the form of EADS in Figure 4A and in the form of DADS in Figure SI 5. Three lifetimes are needed for a sufficient fit of the data: 10 ps, 3.3 ns, and 895 ns. The 10 ps process is assigned to solvation or relaxation, while the 3.3 and 895 ns processes are interpreted as the singlet and triplet lifetime, respectively. The porphyrin singlet lifetime of 3.3 ns is shorter than the fluorescence lifetime of PF_{10}, which is 6.5 ns in benzonitrile as measured by time-resolved fluorescence (Figure SI 16). The most reasonable explanation for this shorter lifetime in Bi-PhOH-PF_{10} is slow photoinduced electron transfer to generate BiH^{+}-$PhO^{\bullet}$-$PF_{10}^{\bullet-}$. This charge separated state is nearly isoenergetic with the porphyrin first excited singlet state, based on results reported previously.[18,20] The spectrum of such a charge separated state is

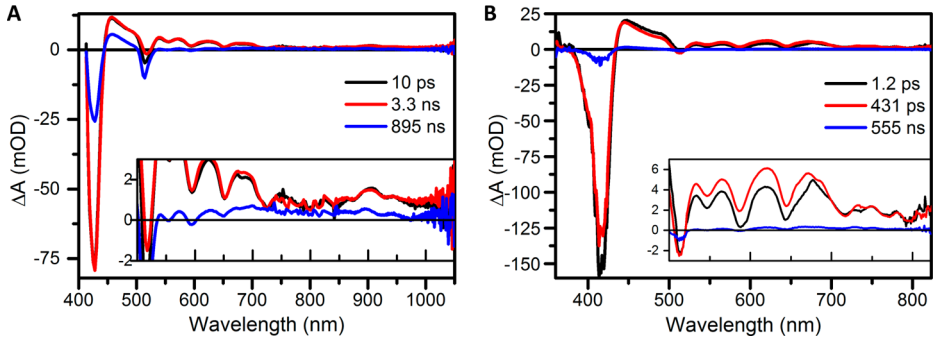

Figure 4. EADS of Bi-PhOH-PF_{10} upon 511 nm excitation. The insets show a magnification of the Δ*A* axis in the 500−1050 nm region: (A) in benzonitrile; (B) in acetonitrile.

DOI: 10.1021/acs.jpcb.5b05298
J. Phys. Chem. B 2015, 119, 12156−12163

not detected, suggesting a recombination process that is faster than charge separation. With this "inverted kinetics" the transient concentration of the charge separated state is too small to be detected. Because the driving force for such a charge separation is extremely small, it is reasonable to assume that charge recombination would be more rapid than charge separation. The triplet yield is estimated at 33%.

Much faster excited state quenching is found in acetonitrile (EADS in Figure 4B and DADS in Figure SI 6) where the corresponding lifetimes are 1.2 ps, 431 ps, and 555 ns. The quenching of the singlet lifetime to 431 ps in combination with a triplet yield of only 6% suggest that charge separation is the dominant decay pathway in acetonitrile. Again, the low concentration of that charge separated state prevents the observation of this spectrum and the recombination rate. The assignment of the 3.3 ns EADS (benzonitrile, Figure 4A) and 431 ps EADS (acetonitrile, Figure 4B) to the relaxed singlet state of the PF_{10} moiety is confirmed by similar values for the fluorescence lifetimes in Figure SI 17.

Triad. We now turn to the Bi-PhOH-PF_{10}-TCNP triad, first in benzonitrile upon 730 nm excitation of the TCNP moiety. The EADS resulting from global analysis is shown in Figure 5

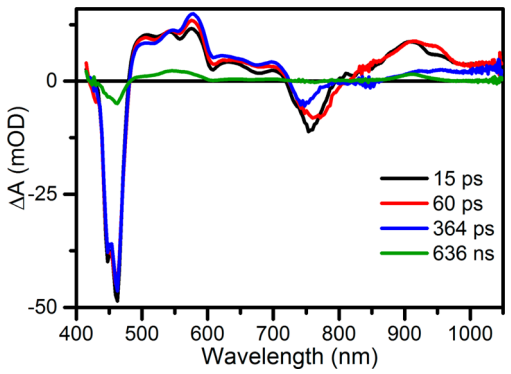

Figure 5. EADS of triad in benzonitrile upon 730 nm excitation.

and the DADS in Figure SI 7. The fast components have lifetimes of 15 and 60 ps and involve spectral changes similar to those shown by TCNP. As for that compound, they can be assigned to solvation and relaxation. The 364 ps EADS closely resembles the 1.7 ns spectrum in Figure 3 and is likewise assigned to the relaxed singlet excited TCNP. The singlet excited-state lifetime of 364 ps is short as compared to that of the TCNP model compound. Because there is little perturbation of the absorption spectra of the two porphyrins upon linking them, the two likely mechanisms for such quenching are in general singlet−singlet energy transfer and photoinduced electron transfer. Singlet energy transfer from TCNP to PF_{10} is precluded because the energy of the TCNP first excited singlet state is much lower than that of PF_{10}. Thus, the most reasonable explanation for the quenching is photoinduced electron transfer from PF_{10} to the first excited singlet state of the attached TCNP. Such electron transfer was also reported in a study of a very similar molecule.[18] On the basis of the lifetime of 1.7 ns found for the decay of TCNP by the usual unimolecular photophysical pathways, we estimate the rate constant for electron transfer to be 2.2×10^9 s^{-1}.

The longest-living EADS of 636 ns has a spectral shape that is very similar to that of the TCNP model triplet state, as is shown in Figure SI 9. Hence, we assign this component to the TCNP triplet state, with a yield of 11%. The spectrum of Bi-PhOH-$PF_{10}^{\bullet+}$-$TCNP^{\bullet-}$ is not detected, and no evidence is found for further charge separation including the Bi-PhOH moiety. We conclude that recombination of Bi-PhOH-$PF_{10}^{\bullet+}$-$TCNP^{\bullet-}$ is sufficiently faster than oxidation of Bi-PhOH by $PF_{10}^{\bullet+}$ so that no BiH^+-$PhO^{\bullet}$-PF_{10}-$TCNP^{\bullet-}$ can be detected at our signal-to-noise level.

The photophysics of the triad in acetonitrile (Figure SI 8) upon excitation of the TCNP moiety shows solvation and relaxation processes with 1.2 and 12 ps constants, a singlet excited-state lifetime of 739 ps, and a triplet lifetime of 634 ns, without evidence for long-lived charge separated states. The quenching of the singlet lifetime to 739 ps again indicates charge separation to form Bi-PhOH-$PF_{10}^{\bullet+}$-$TCNP^{\bullet-}$ and fast recombination.

Table 1 summarizes the results obtained from global analysis. For Bi-PhOH-PF_{10} and triad quenched singlet lifetimes are found in both benzonitrile and acetonitrile, most likely indicating charge transfer processes. Recombination time scales cannot be resolved due to inverted kinetics.

Table 1. Lifetimes, Triplet Yields, and Electron Transfer Signals Resulting from Global Analysis of the Transient Absorption Spectroscopy Data[a]

compd	solvent	singlet lifetime	triplet lifetime	triplet yield[b] (%)	electron transfer
TCNP	benzonitrile	1.7 ns	698 ns	37	–
TCNP	acetonitrile	1.2 ns	524 ns	39	–
Bi-PhOH-PF10	benzonitrile	3.3 ns	895 ns	33	yes
Bi-PhOH-PF10	acetonitrile	431 ps	555 ns	6	yes
triad	benzonitrile	364 ps	636 ns	11	yes
triad	acetonitrile	739 ps	634 ns	26	yes

[a]The triad was excited at the TCNP moiety. [b]Estimated from the amplitude of the Soret band bleach.

The results obtained for the triad are different than those reported previously by Megiatto et al. for a related triad which has two *tert*-butyl groups at the 3,5-positions of each of three of the *meso*-phenyl groups on the TCNP moiety, instead of a single *tert*-butyl group at the 4-position of each of three of the *meso*-phenyl groups of TCNP.[18] In the earlier system, Bi-PhOH-PF_{10}-^{1}TCNP in benzonitrile decayed with a time constant of 590 ps to yield Bi-PhOH-$PF_{10}^{\bullet+}$-$TCNP^{\bullet-}$. This state, which recombined in 12 ps in a related dyad, evolved into a final BiH^+-$PhO^{\bullet}$-PF_{10}-$TCNP^{\bullet-}$ state, which was formed with an estimated quantum yield of about 50% and had a lifetime of 3.8 μs. The estimated yield of BiH^+-$PhO^{\bullet}$-PF_{10}-$TCNP^{\bullet-}$ was based on the assumption that the yields of triplet in triad **1** and dyad **2** in that paper were identical. Re-examination of the data shows that due to the impurities or alternate conformations referred to in ref 18, this assumption was not valid, and the quantum yield is likely substantially lower than originally estimated.

Nonetheless, these two closely related triads differ in electron transfer behavior in that the earlier triad demonstrates formation of the BiH^+-$PhO^{\bullet}$-PF_{10}-$TCNP^{\bullet-}$ state, while in the present triad the Bi-PhOH-$PF_{10}^{\bullet+}$-$TCNP^{\bullet-}$ state recombines too rapidly for detectable formation of a BiH^+-$PhO^{\bullet}$-PF_{10}-$TCNP^{\bullet-}$ species. The difference in behavior of these two very similar triads must be related to the structural differences in the TCNP moieties. Such differences will affect the molecular conformation (and therefore electronic coupling between the

DOI: 10.1021/acs.jpcb.5b05298
J. Phys. Chem. B 2015, 119, 12156−12163

moieties[34]), the thermodynamic driving force, and the internal and solvent reorganization energy for the various electron transfer steps. Although we do not know the relative contributions of these factors to the behavior of the molecules, the results show that such effects are present. For example, the lifetime of the relaxed Bi-PhOH-PF_{10}-^{1}TCNP in the earlier triad is 610 ps, whereas in the present triad, it is only 364 ps. Thus, the initial photoinduced electron transfer to form Bi-PhOH-$PF_{10}^{\bullet+}$-$TCNP^{\bullet-}$ occurs almost twice as rapidly in the present triad. Evidently, in the present triad recombination of Bi-PhOH-$PF_{10}^{\bullet+}$-$TCNP^{\bullet-}$ is also faster than it is in the earlier triad, and this precludes observation of a charge shift to form BiH^+-$PhO^\bullet$-PF_{10}-$TCNP^{\bullet-}$. Although the structural differences would be expected to be subtle, their effect on electron transfer rates and yields is evidently substantial.

It is unlikely that driving forces for the two triads are very different, as cyclic voltammetric measurements on the acid form of TCNP and 7,8,17,18-tetracyano-5-(4-carboxyphenyl)-10,15,20-tris(3,5-di-*tert*-butylphenyl)porphyrin in dichloromethane give identical results within experimental error for the first reduction potential (−0.26 V vs SCE in Figure SI 18, compared to −0.30 V reported by Megiatto et al.[18]). Given this fact, changes in reorganization energy that would increase the rate of photoinduced electron transfer in the current Bi-PhOH-PF_{10}-^{1}TCNP relative to the triad reported earlier (due to shifting the reaction in the normal region of the Marcus rate vs free energy change relationship toward the maximum rate) would also be expected to shift the charge recombination reaction of the current Bi-PhOH-$PF_{10}^{\bullet+}$-$TCNP^{\bullet-}$ more into the Marcus inverted region, thereby slowing its rate relative to that of the earlier triad. This is not observed. Thus, the most likely explanation for the difference in behavior of the two molecules is an increase in electronic coupling in the current Bi-PhOH-PF_{10}-TCNP compared to the earlier triad. For example, a small change in conformation about the amide linkage between the two porphyrins or electronic effects due to the differences in phenyl substituents could cause such a change.

For the current triad, the decrease in the rate constant for photoinduced electron transfer on changing solvent from benzonitrile to acetonitrile, about a factor of 2, indicates a strong sensitivity of electron transfer to changes in solvation. However, from limited kinetic studies in these two solvents, and the *caveat* that benzonitrile provides an additional level of solvation due to quadrupole interactions arising from the aromatic ring,[35] only qualitative observations about the role of solvation in these systems can be made. The solvent reorganization energy of acetonitrile is larger than that of benzonitrile[36] (but note that the static dielectric constant favors benzonitrile), which would slow photoinduced electron transfer in acetonitrile, as observed. This effect would also be expected to increase the rate of charge recombination (occurring in the Marcus inverted region). Solvent stabilization of the ion pair is expected to be weaker in acetonitrile relative to benzonitrile.[35] This would result in less driving force for photoinduced electron transfer, and therefore a smaller rate constant in acetonitrile, as observed. This effect would also be expected to slow charge recombination, but it is evidently not enough to give a detectable yield of the final BiH^+-$PhO^\bullet$-PF_{10}-$TCNP^{\bullet-}$ species.

In the case of Bi-PhOH-PF_{10}, the driving force and reorganization energy effects upon changing solvent from benzonitrile to acetonitrile might be expected to decrease the rate of photoinduced electron transfer from Bi-PhOH-$^1PF_{10}$ to yield BiH^+-$PhO^\bullet$-$PF_{10}^{\bullet-}$, for the reasons discussed above. However, electron transfer is considerably more rapid in acetonitrile. This difference might be related to stronger hydrogen-bonding interactions that facilitate PCET in acetonitrile[20] and/or to changes in electronic coupling resulting from conformational changes.

CONCLUSION

In summary, we report the synthesis and time-resolved spectroscopic analysis of a Bi-PhOH-PF_{10}-TCNP triad and related compounds. In the triad, the singlet lifetime of the TCNP moiety is found to be 364 ps in benzonitrile and 739 ps in acetonitrile, compared to 1.7 and 1.2 ns, respectively, for the TCNP reference molecule. This quenching of the singlet lifetime is assigned to electron transfer from PF_{10} to ^{1}TCNP. The rate constant for photoinduced electron transfer in the triad is substantially larger than was reported for a similar triad, and the long-living charge separated state detected for that triad was not found in the current system. These observations in the context of the small structural differences between the triads show that the system is extremely sensitive to small structural changes. The system is also very sensitive to small environmental changes, as illustrated by the large differences in photoinduced electron transfer rate constants for the triad and a related dyad upon changing the solvent from benzonitrile to acetonitrile.

ASSOCIATED CONTENT

Supporting Information

The Supporting Information is available free of charge on the ACS Publications website at DOI: 10.1021/acs.jpcb.5b05298.

^{1}H NMR, additional steady-state, transient absorption, and time-resolved fluorescence spectroscopy and electrochemistry (PDF)

AUTHOR INFORMATION

Corresponding Author

*E-mail j.t.m.kennis@vu.nl; Ph +31 205987212; Fax +31 20 5987999 (J.T.M.K.).

Present Addresses

J.D.M.: Institute of Chemistry, Campinas State University (UNICAMP), Campinas, SP, 13084-861, Brazil.

D.D.M.-H.: Department of Chemistry, Yale University, New Haven, CT 06511.

Notes

The authors declare no competing financial interest.

ACKNOWLEDGMENTS

J.R. was supported by the research programme of BioSolar Cells, cofinanced by the Dutch Ministry of Economic Affairs. Work at Arizona State University was supported by the Office of Basic Energy Sciences, Division of Chemical Sciences, Geosciences, and Energy Biosciences, Department of Energy, under Contract DE-FG02-03ER15393. J.T.M.K. was supported by a VICI grant of the Chemical Sciences council of The Netherlands Organization of Scientific Research (NWO−CW). R.N.F. was supported by a VIDI grant of the Earth and Life Sciences Council of The Netherlands. R. v. G. was supported by the VU University Amsterdam, the Laserlab-Europe Consortium and by the EU FP7 project PAPETS (GA 323901). R.v.G. gratefully acknowledges his Academy Professor

DOI: 10.1021/acs.jpcb.5b05298
J. Phys. Chem. B 2015, 119, 12156−12163

grant from the Netherlands Royal Academy of Sciences (KNAW).

REFERENCES

(1) Blankenship, R. E. *Molecular Mechanisms of Photosynthesis*; Blackwell Science Ltd.: Hoboken, NJ, 2001; p 336.

(2) Hammarström, L.; Styring, S. Proton-coupled electron transfer of tyrosines in Photosystem II and model systems for artificial photosynthesis: the role of a redox-active link between catalyst and photosensitizer. *Energy Environ. Sci.* **2011**, *4* (7), 2379.

(3) Migliore, A.; Polizzi, N. F.; Therien, M. J.; Beratan, D. N. Biochemistry and theory of proton-coupled electron transfer. *Chem. Rev.* **2014**, *114* (7), 3381−3465.

(4) Cox, N.; Pantazis, D. A.; Neese, F.; Lubitz, W. Biological water oxidation. *Acc. Chem. Res.* **2013**, *46* (7), 1588−1596.

(5) Noguchi, T. Fourier transform infrared difference and time-resolved infrared detection of the electron and proton transfer dynamics in photosynthetic water oxidation. *Biochim. Biophys. Acta, Bioenerg.* **2015**, *1847* (1), 35−45.

(6) Fukuzumi, S. Bioinspired electron-transfer systems and applications. *Bull. Chem. Soc. Jpn.* **2006**, *79* (2), 177−195.

(7) Berera, R.; Herrero, C.; van Stokkum, I. H. M.; Vengris, M.; Kodis, G.; Palacios, R. E.; van Amerongen, H.; van Grondelle, R.; Gust, D.; Moore, T. A.; et al. A simple artificial light-harvesting dyad as a model for excess energy dissipation in oxygenic photosynthesis. *Proc. Natl. Acad. Sci. U. S. A.* **2006**, *103* (14), 5343−5348.

(8) Kloz, M.; Pillai, S.; Kodis, G.; Gust, D.; Moore, T. A.; Moore, A. L.; van Grondelle, R.; Kennis, J. T. M. Carotenoid photoprotection in artificial photosynthetic antennas. *J. Am. Chem. Soc.* **2011**, *133* (18), 7007−7015.

(9) Guldi, D. M. Fullerene−porphyrin architectures; photosynthetic antenna and reaction center models. *Chem. Soc. Rev.* **2002**, *31* (1), 22−36.

(10) Pillai, S.; Ravensbergen, J.; Antoniuk-Pablant, A.; Sherman, B. D.; van Grondelle, R.; Frese, R. N.; Moore, T. A.; Gust, D.; Moore, A. L.; Kennis, J. T. M. Carotenoids as electron or excited-state energy donors in artificial photosynthesis: an ultrafast investigation of a carotenoporphyrin and a carotenofullerene dyad. *Phys. Chem. Chem. Phys.* **2013**, *15* (13), 4775−4784.

(11) Gust, D.; Moore, T. A.; Moore, A. L. Realizing artificial photosynthesis. *Faraday Discuss.* **2012**, *155*, 9−26.

(12) Barry, B. A. Reaction dynamics and proton coupled electron transfer: Studies of tyrosine-based charge transfer in natural and biomimetic systems. *Biochim. Biophys. Acta, Bioenerg.* **2015**, *1847* (1), 46−54.

(13) Rhile, I. J.; Markle, T. F.; Nagao, H.; DiPasquale, A. G.; Lam, O. P.; Lockwood, M. A.; Rotter, K.; Mayer, J. M. Concerted proton−electron transfer in the oxidation of hydrogen-bonded phenols. *J. Am. Chem. Soc.* **2006**, *128* (18), 6075−6088.

(14) Mayer, J. M.; Rhile, I. J.; Larsen, F. B.; Mader, E. A.; Markle, T. F.; DiPasquale, A. G. Models for Proton-coupled electron transfer in photosystem II. *Photosynth. Res.* **2006**, *87* (1), 3−20.

(15) Concepcion, J. J.; Brennaman, M. K.; Deyton, J. R.; Lebedeva, N. V.; Forbes, M. D. E.; Papanikolas, J. M.; Meyer, T. J. Excited-state quenching by proton-coupled electron transfer. *J. Am. Chem. Soc.* **2007**, *129* (22), 6968−6969.

(16) Lachaud, F.; Quaranta, A.; Pellegrin, Y.; Dorlet, P.; Charlot, M.-F.; Un, S.; Leibl, W.; Aukauloo, A. A Biomimetic model of the electron transfer between P680 and the TyrZ−His190 pair of PSII. *Angew. Chem., Int. Ed.* **2005**, *44* (10), 1536−1540.

(17) Reece, S. Y.; Hodgkiss, J. M.; Stubbe, J.; Nocera, D. G. Proton-coupled electron transfer: the mechanistic underpinning for radical transport and catalysis in biology. *Philos. Trans. R. Soc., B* **2006**, *361* (1472), 1351−1364.

(18) Megiatto, J. D.; Antoniuk-Pablant, A.; Sherman, B. D.; Kodis, G.; Gervaldo, M.; Moore, T. A.; Moore, A. L.; Gust, D. Mimicking the electron transfer chain in photosystem II with a molecular triad thermodynamically capable of water oxidation. *Proc. Natl. Acad. Sci. U. S. A.* **2012**, *109* (39), 15578−15583.

(19) Megiatto, J. D.; Patterson, D.; Sherman, B. D.; Moore, T. A.; Gust, D.; Moore, A. L. Intramolecular hydrogen bonding as a synthetic tool to induce chemical selectivity in acid catalyzed porphyrin synthesis. *Chem. Commun.* **2012**, *48* (38), 4558−4560.

(20) Megiatto, J. D., Jr.; Méndez-Hernández, D. D.; Tejeda-Ferrari, M. E.; Teillout, A.-L.; Llansola-Portolés, M. J.; Kodis, G.; Poluektov, O. G.; Rajh, T.; Mujica, V.; Groy, T. L.; et al. A bioinspired redox relay that mimics radical interactions of the Tyr−His pairs of photosystem II. *Nat. Chem.* **2014**, *6* (5), 423−428.

(21) Moore, G. F.; Hambourger, M.; Gervaldo, M.; Poluektov, O. G.; Rajh, T.; Gust, D.; Moore, T. A.; Moore, A. L. A Bioinspired construct that mimics the proton coupled electron transfer between P680●+ and the TyrZ-His190 pair of photosystem II. *J. Am. Chem. Soc.* **2008**, *130* (32), 10466−10467.

(22) Moore, G. F.; Megiatto, J. D.; Hambourger, M.; Gervaldo, M.; Kodis, G.; Moore, T. A.; Gust, D.; Moore, A. L. Optical and electrochemical properties of hydrogen-bonded phenol-pyrrolidino[60]fullerenes. *Photochem. Photobiol. Sci.* **2012**, *11* (6), 1018.

(23) Chumakov, D. E.; Khoroshutin, A. V.; Anisimov, A. V.; Kobrakov, K. I. Bromination of porphyrins (Review). *Chem. Heterocycl. Compd.* **2009**, *45* (3), 259−283.

(24) Ravensbergen, J.; Abdi, F. F.; van Santen, J. H.; Frese, R. N.; Dam, B.; van de Krol, R.; Kennis, J. T. M. Unraveling the carrier dynamics of $BiVO_4$: A femtosecond to microsecond transient absorption study. *J. Phys. Chem. C* **2014**, *118* (48), 27793−27800.

(25) Berera, R.; van Grondelle, R.; Kennis, J. T. M. Ultrafast transient absorption spectroscopy: principles and application to photosynthetic systems. *Photosynth. Res.* **2009**, *101*, 105−118.

(26) Snellenburg, J. J.; Laptenok, S.; Seger, R.; Mullen, K. M.; van Stokkum, I. H. M. Glotaran: A java-based graphical user interface for the R package TIMP. *J. Stat. Software* **2012**, *49* (3), 22.

(27) van Stokkum, I. H. M.; Larsen, D. S.; van Grondelle, R. Global and target analysis of time-resolved spectra. *Biochim. Biophys. Acta, Bioenerg.* **2004**, *1657* (2−3), 82−104.

(28) van Stokkum, I. H. M.; Larsen, D. S.; van Grondelle, R. Erratum to "Global and target analysis of time-resolved spectra" [*Biochim. Biophys. Acta* **2004**, *1658* (2−3), 82−104]. *Biochim. Biophys. Acta* **2004**, *1658* (3).

(29) Kennis, J. T. M.; Groot, M.-L. Ultrafast spectroscopy of biological photoreceptors. *Curr. Opin. Struct. Biol.* **2007**, *17* (5), 623−630.

(30) Papagiannakis, E.; Kennis, J. T. M.; van Stokkum, I. H. M.; Cogdell, R. J.; van Grondelle, R. An alternative carotenoid-to-bacteriochlorophyll energy transfer pathway in photosynthetic light harvesting. *Proc. Natl. Acad. Sci. U. S. A.* **2002**, *99* (9), 6017−6022.

(31) Bonetti, C.; Alexandre, M. T. A.; van Stokkum, I. H. M.; Hiller, R. G.; Groot, M. L.; van Grondelle, R.; Kennis, J. T. M. Identification of excited-state energy transfer and relaxation pathways in the peridinin-chlorophyll complex: an ultrafast mid-infrared study. *Phys. Chem. Chem. Phys.* **2010**, *12* (32), 9256−9266.

(32) Toh, K. C.; Stojkovic, E. A.; van Stokkum, I. H.; Moffat, K.; Kennis, J. T. Fluorescence quantum yield and photochemistry of bacteriophytochrome constructs. *Phys. Chem. Chem. Phys.* **2011**, *13* (25), 11985−11997.

(33) Sazanovich, I. V.; Galievsky, V. A.; van Hoek, A.; Schaafsma, T. J.; Malinovskii, V. L.; Holten, D.; Chirvony, V. S. Photophysical and structural properties of saddle-shaped free Base porphyrins: Evidence for an "Orthogonal" dipole moment. *J. Phys. Chem. B* **2001**, *105* (32), 7818−7829.

(34) Migliore, A.; Corni, S.; Varsano, D.; Klein, M. L.; Di Felice, R. First principles effective electronic couplings for hole transfer in natural and size-expanded DNA. *J. Phys. Chem. B* **2009**, *113* (28), 9402−9415.

(35) Horng, M. L.; Gardecki, J. A.; Papazyan, A.; Maroncelli, M. Subpicosecond measurements of polar solvation dynamics: Coumarin 153 Revisited. *J. Phys. Chem.* **1995**, *99* (48), 17311−17337.

(36) Reynolds, L.; Gardecki, J. A.; Frankland, S. J. V.; Horng, M. L.; Maroncelli, M. Dipole solvation in nondipolar solvents: Experimental

DOI: 10.1021/acs.jpcb.5b05298
J. Phys. Chem. B 2015, 119, 12156−12163

studies of reorganization energies and solvation dynamics. *J. Phys. Chem.* **1996**, *100* (24), 10337−10354.

DOI: 10.1021/acs.jpcb.5b05298
J. Phys. Chem. B 2015, 119, 12156−12163